THE ROLE OF NIOBIUM IN WROUGHT SUPERALLOYS

S. J. Patel and G. D. Smith

Special Metals Corporation
3200 Riverside Drive
Huntington, WV 25705-1771, U.S.A.

Abstract

It is the purpose of this paper to examine the role that niobium plays in certain superalloys and to describe the properties that are achieved as a result of its inclusion in these wrought superalloys. To begin, the general alloying characteristics of niobium in nickel-base alloys are described. Then the specific role of niobium in the alloys 625, 706 and 718 is examined for its contribution to developing microstructure and the impact of the resulting microstructure on properties. This paper defines the role the niobium plays in making these alloys premier materials of choice in today's aerospace and land-based gas turbines.

Introduction

Niobium is recognized as a key alloying element in a number of major nickel-base wrought superalloys. It is the purpose of this paper to examine the role that niobium plays in these alloys and describe the properties that are achieved as a result of its inclusion in wrought superalloys. Besides the general alloying characteristics of niobium as described in the technical literature, the specific role of this element in the alloys 625, 706 and 718 will be examined. Niobium in these alloys will be assessed for the role it plays in developing microstructure and the impact of the resulting microstructure on properties.

Alloys 625, 706 and 718 fit the definition of a superalloy in that they are alloys developed for elevated temperature service, where severe mechanical stress is encountered and high surface integrity is usually required. These three superalloys are commonly considered to be nickel-base alloys although alloys 706 and 718 contain significant levels of iron to reduce the cost of these alloys intended for such applications as large forgings. It seems appropriate to begin by examining the relevant properties of the element, niobium, as it pertains to its use in superalloys. In our alloys of interest, niobium is present in small-to-moderate amounts and contributes in a significant way to alloy properties. As alloys generally intended for gas turbine service, these alloys must meet stringent criteria for tensile strength and ductility, rupture and creep strength with inherent stability and ductility, favorable low-cycle fatigue requirements and even requirements on density, thermal conductivity and expansion characteristics. This paper will seek to define the role that niobium plays in making these alloys premier materials of choice in today's aerospace and land-based gas turbines.

The Elemental Properties of Niobium

Niobium, a body-centered cubic (BCC) Group VA element, is one of the four major refractory elements used in superalloys along with molybdenum (also found in alloys 625 and 718 along with niobium), tungsten and tantalum. These alloying elements, added singularly or in combination, contribute to solid solution strengthening, strengthening through carbide formation and in the case of niobium to precipitation hardening as well. Niobium, as a refractory element, is of lower modulus, melting point and density than the other refractory elements. See Table I. Since effective solid solution hardening is suggested by high modulus and high melting point, it is clear that niobium is not as effective in solid solution hardening as the other refractory elements.

Table I Selected physical properties of the refractory elements, niobium, molybdenum, tantalum and tungsten

	Nb	Mo	Ta	W
Melting Point, °C	2468	2610	2996	3410
Density, g/cm^3	8.4	10.2	16.6	19.3
Modulus, n/m^2 x 10^6	100	345	185	345
Atomic Radii, å	2.852	2.720	2.854	2.735

Atomic size as presented in Table I can contribute to solid solution strengthening as it influences relative solubility. Table II shows niobium to be the least soluble refractory element in nickel and nickel-20% chromium. The atomic mismatch of niobium with nickel and iron is the greatest of the refractory elements. Mismatch certainly contributes to limiting solubility. This is also shown in Table II.

Table II Factors influencing solid solution strengthening by the refractory elements in nickel and nickel-20% chromium matrices

Solubility Limit At 1000-1200°C Wt % in	Solvate Element			
	Nb	Mo	Ta	W
Ni	10	26	12	17
Ni-20% Cr	7	23	12	33

Atom Size Mismatch Wt % vs.	Solvate Element			
	Nb	Mo	Ta	W
Fe	10.8	5.7	10.6	6.3
Ni	14.7	9.4	14.4	10.0

Niobium is the most electropositive of the four refractory elements. This electropositive characteristic defines why niobium has a strong affinity for the formation of A_3B-type TCP phases. Niobium substitutes for aluminum in γ' (Ni_3Al) as does titanium. Niobium also forms γ'' (Ni_3Nb), the body-centered tetragonal (BCT) strengthener phase, in alloys 706 and 718. The electropositive nature of niobium favors NbC (-ΔF = 30 Kcal/g-atom) and NbN (-ΔF = 38 Kcal/g-atom), usually present to some extent as primary or secondary phases in alloys 625, 706 and 718. Carbon and nitrogen can combine to form primary and secondary Nb(C,N) as well. Niobium has a moderate affinity for oxygen forming Nb_2O_5 [1/5 Nb_2O_5 (-ΔF = 38 Kcal/g-atom)].

It has already been stated that niobium has the potential to strengthen a nickel-base alloy by solid solution strengthening, carbide formation and by coherent precipitation hardening phase formation. Let us look at each of these strengthening mechanisms in turn with niobium in mind.

Solid Solution Strengthening with Niobium in Nickel-Base Superalloys

Foreign atom substitution in a lattice can cause strain by lattice expansion, which in turn interacts with dislocations. As presented in Table I, niobium does not dissolve extensively in nickel or nickel-20% chromium alloys. It is limited to about 7% in nickel-20% chromium at 1200°C and becomes less with decreasing temperature. Atomic size mismatch at about 15% with respect to nickel is too large to allow greater solubility. However, this size mismatch does imply a potential for a measurable effect per niobium atom in creating lattice strain. An early study of the effect of niobium in nickel-20% chromium is of immense value in understanding the solid solution effects of niobium in the three alloys of this paper.

Guo and Ma studied the behavior of niobium in a nickel-20% chromium matrix slightly strengthened with γ' and carbon (1). These investigators vacuum melted this matrix base with eight levels of niobium from 0% to 2.4%. Following fabrication of bar, the compositions were solution heat treated at 1080°C/8h/AC and subsequently aged at 750°C/16h/AC. The authors then proceeded to separate the phases and analyze them for alloy content and lattice spacing, measure particle sizes, determine volume fraction of γ', mismatch and the long range order parameter, S. Room Temperature tensile data were also obtained and the yield strength increase for the incremental additions of niobium were determined and assessed for their contribution to strengthening. Table III summarizes their results.

Figure 1 depicts the partitioning of niobium to the various phases found, i.e., γ, γ' and the carbides. At any given niobium content, the bulk of the niobium partitions to the γ (~57%) followed by partitioning to γ' (~28%) and least to the carbides (~15%). These authors found niobium increased the lattice spacing of γ slightly from 3.5634 nm at 0% niobium to 3.5713 nm at 2.46% niobium. Lattice mismatch of γ to γ' increased from 0.76 in the niobium-free composition to 0.81 at 1.24% niobium and then decreased to the original mismatch value at 2.46% niobium. The shear modulus increased from 81.7 x 10^3 to 85.0 x 10^3 over the range of niobium content studied. Guo and Ma have confirmed a solid solution strengthening effect for niobium that is germane to alloys 625, 706 and 718 containing 20% chromium in their nickel and nickel-iron matrices. Their estimate is that the yield strength had been increased by ~44 MPa due to solid solution strengthening by the addition of 2.46% niobium. This is roughly one half of the total room temperature yield strength increase attributed to the addition of the niobium. Because the mismatch between the γ and γ' phases did not significantly change with increasing niobium content, it was concluded that niobium's contribution to coherency strain due to mismatch is small. See Table III. Hence the addition of niobium does not raise strength through increasing coherency strain via mismatch. The balance of the strength increase in their alloys was attributed principally to coherency strain strengthening through the role of niobium in increasing APB energy of the alloys.
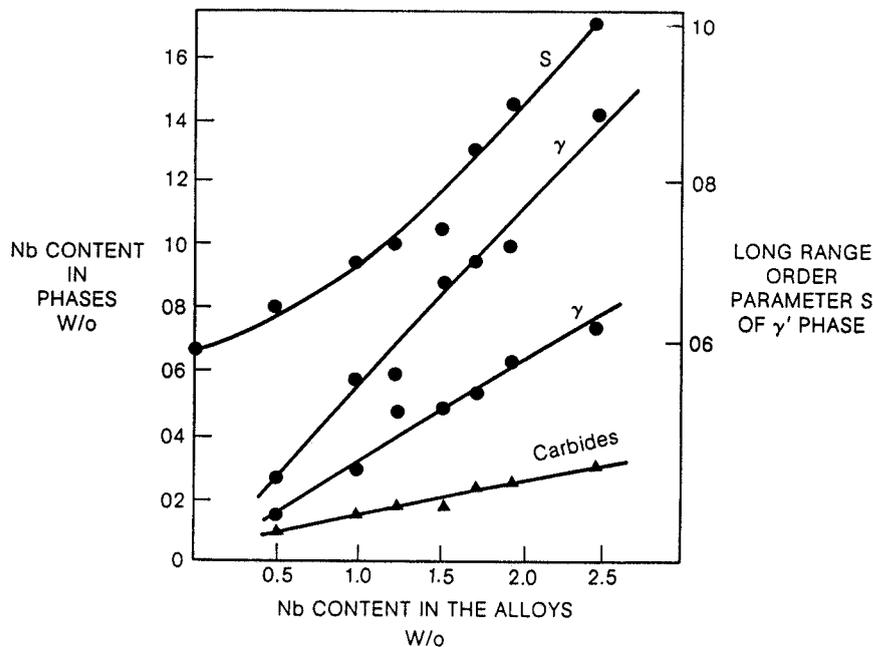

Figure 1: Partitioning of niobium to γ, γ' and the carbides along with the long-range order parameter "S" of γ' in solid solution nickel-base alloys containing 0 to 2.5% niobium (1).

Table III. Niobium Behavior in Experimental Ni-Base Austenitic Superalloys [Guo and Ma (1)].

Heat No	Nb Content In the alloys	γ'Content Wt%						Carbide Content Wt%		
		Ni	Cr	Nb	Al	Ti	Total	Ni	Ti	Nb
1	--	9.46	0.222	--	0.666	1.387	11.74	<0.01	0.023	--
2	0.51	9.40	0.467	0.138	0.710	1.404	12.12	0.01	0.066	0.103
3	1.00	10.40	0.532	0.291	0.710	1.427	13.36	0.01	0.063	0.140
4	1.24	10.75	0.554	0.469	0.702	1.475	13.95	0.01	0.055	0.181
5	1.53	10.80	0.551	0.485	0.705	1.476	14.02	0.01	0.054	0.170
6	1.72	10.90	0.547	0.529	0.700	1.481	14.15	0.01	0.069	0.246
7	1.94	11.70	0.608	0.628	0.710	1.489	15.14	0.01	0.061	0.246
8	2.46	11.80	0.580	0.739	0.745	1.522	15.39	0.01	0.058	0.301

Heat No.	Lattice Spacing Å		Mismatch ε, %	Particle Radius r, Å	Long Range Order Parameter, S	Volume Fraction of γ' %
	γ'	γ				
1	35.906	35.634	0.76	84.5	0.79	12.56
2	35.933	35.666	0.75	85.5	0.82	12.98
3	35.951	35.671	0.78	98.5	0.85	14.18
4	35.965	35.674	0.81	101.5	0.86	14.85
5	35.967	35.682	0.80	98.5	0.87	14.84
6	35.970	35.701	0.75	98.5	0.92	14.95
7	35.976	35.701	0.77	105	0.95	15.91
8	35.987	35.713	0.77	113	1.01	16.21

Room Temperature Tensile Properties			Calculated Solid Solution Strengthening and APB Values Due to Nb Additions		
0.2% Y.S. MPa	U.T.S. MPa	Incremental Increase In 0.2%Y.S. MPa	Δ Solid Solution Strengthening by Nb 0.2% Y.S., MPa	APB Energy J/m²	0.2% Yield Strength Incremental Increase By APB, MPa
743	1062	--	--	119.9×10^{-3}	--
783	1175	40	18	129.0×10^{-3}	4
784	1206	41	21	138.5×10^{-3}	12
816	1203	73	23	141.6×10^{-3}	14
816	1216	73	26	144.9×10^{-3}	14
830	1229	87	37	162.0×10^{-3}	23
834	1242	91	37	172.7×10^{-3}	31
826	1268	83	44	191.3×10^{-3}	46

Carbide Strengthening by Niobium in Nickel-Base Superalloys

Carbides, in general, are particularly useful in aiding structural refinement during fabrication and heat treatment by assisting in grain size control. They strengthen the matrix when present intragranularly and aid high temperature strength by inhibiting slip in grain boundaries. Conversely, carbides can also be a source at which dislocations are generated and fatigue cracks are initiated. Among the carbides, niobium usually forms MC type carbide in the as-cast and hot worked conditions. During subsequent thermal exposure, the MC type carbide might be expected to degenerate into chromium-containing $M_{23}C_6$ type carbide by way of the following reaction:

$$MC + \gamma = M_{23}C_6 + \gamma' \tag{1}$$

This reaction has been documented by Mihalisin in a 2% niobium-containing cast alloy 713C (2). Niobium is believed to retard the reaction rate of MC type carbides to $M_{23}C_6$ type carbides. Beattie speculates that the stability of the MC type carbides decreases in the following order – TaC>NbC>TiC>VC (3). Sims reports that niobium is about equal to tantalum in stabilizing MC type carbides (4). Molybdenum is believed to destabilize NbC (5). Guo and Ma reported in their study that ~15% of the niobium content partitioned to the carbide phase, assumed to be MC type carbides.

Alloy X-750, while not an alloy under scrutiny in this paper, does contain 1% niobium. The partitioning of niobium to the $M_{23}C_6$ in this alloy has been studied by E. L. Raymond (6). This author finds that the element in greatest abundance in the $M_{23}C_6$ that forms between 650°C and 930°C is niobium followed by titanium and finally by chromium. The levels of niobium are initially in the 60 to 70% range and gradually decrease as low as the mid-40s as chromium displaces both niobium and titanium in the carbide. At temperatures above ~820°C, the $M_{23}C_6$ type carbides is devoid of chromium and consists of 30% titanium, 70% niobium and 0.18%C. This establishes a role for niobium in aiding stabilization of an alloy against sensitization given a proper heat treatment. For alloy 750, a heat treatment between 820°C and 930°C assures that the zone immediately adjacent to the carbide lamellae retains its chromium content, thereby inhibiting the solution of γ'. This action eliminates a zone of lower strength along the grain boundaries that could potentially lower rupture life and favor crack growth.

Coherent Phase Strengthening by Niobium in Nickel-Base Superalloys

The most significant strengthening mechanism in nickel-base alloys is precipitation strengthening from γ' (Ni_3Al). This phase causes strengthening through generation of coherency strains with the matrix lattice via its effect on APB (antiphase boundary) energy in dislocation cutting, strength and size of the γ' and other factors. Gamma prime allows substitution by niobium and titanium for aluminum and substitution of chromium and cobalt for nickel. Mihalisin found niobium substituted for about 10% of the aluminum in cast alloy 713C (2). Kriege and Baris in analyzing a series of superalloys found niobium to substitute for about 12% of the aluminum in γ' (7). Adding niobium to a γ'-containing alloy can increase the amount of γ' and change its stability as well. Importantly, Thornton et al. found that niobium as well as titanium doubled the flow strength of γ' at typical superalloy service temperature, i.e., 600°C to 900°C (8). See Figure 2.
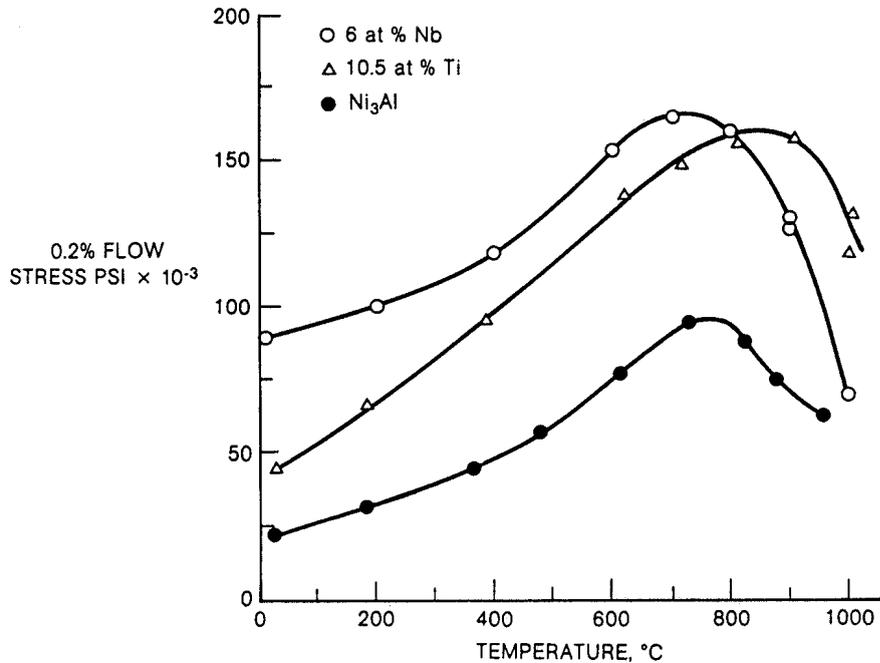
Figure 2: Effect of alloying with niobium and titanium on the flow stress of γ' (8).

The study of Guo and Ma is especially relevant with respect to γ' strengthening (1). These investigators found that niobium partitioned to the γ' in approximately 1:2 to that found in the matrix as shown in Figure 1. As the niobium content increased from 0% to 2.46%, the amount of γ' increased 30% from 12.56% to 16.21%, while lattice mismatch initially increased from 0.76 to 0.81 at 1.24% niobium and back to 0.77 at 2.46% niobium. Niobium increases the amount of γ' both by contributing to its formation and also by decreasing the solubility of aluminum and titanium in the matrix, which in turn can further increase the amount of γ'. Guo and Ma in their study found that lattice mismatch caused by niobium contributed little to coherency strain and hence to yield strength increase. Utilizing the values of long-range order that increased with increasing niobium content, they calculated that the APB energy had increased 60% over that of the niobium-free composition. See Table III. They thus attributed about half the increase in yield strength associated with increasing niobium content to the increase in APB energy.

At this point, one can now begin to speculate what might be the role of niobium in alloys 625, 706 and 718. Niobium's moderate melting point and low modulus seem to indicate little potential for solid solution strengthening. Niobium's large atomic radius limits solubility in nickel alloys and its electropositive nature suggest a bias towards formation of stable carbides and nitrides. Its low density is a potential plus for a superalloy, particularly, if the alloy is to be used for a rotating part. Niobium's greatest potential lies in its ability to promote formation of γ' and γ''. It tends to segregate to these two phases thus increasing their volume faction, while reducing the solubility of aluminum and titanium in the matrix, thereby further increasing the γ' and γ'' contents. Additionally, niobium is known to increase the APB energy of γ' thus increasing high temperature strength through enhancement of increasing resistance to dislocation cutting.

With this cursory level of understanding of the characteristics of niobium, one can now begin to examine the role of niobium in the three alloys selected for this paper. This assessment will begin with alloy 625, the most nickel-rich of the three alloys under study here. The nominal composition of all three alloys is presented in Table IV.

Table IV Nominal composition of the three key alloys of this paper

Alloy	Ni	Fe	Cr	Mo	Al	Ti	Nb	Si	C
625	61.0	2.5	21.5	9.0	0.2	0.2	3.6	0.25	0.02
706	41.5	40.0	16.0	---	0.2	0.2	2.9	0.18	0.01
718	52.5	19.0	19.0	3.0	0.5	0.9	5.3	---	0.04

Metallurgical Behavior of Niobium in Alloy 625

This alloy was introduced commercially in the early 1960s for the intended use as high strength super critical steam boiler tubing. Applications envisioned since product introduction have been principally in the aerospace, chemical process and marine industries. Within aerospace, the alloy has been widely used as thrust reversers, hush kits, cowling, bleed air ducting, combustors, transition ducting, exhaust components and engine mounting flanges and brackets. Over the years, property optimization has led to new commercial alloys, such as, alloys 725 and Custom Age 625Plus[®] (increased strength through increased titanium additions), alloy 626 (increased carburization resistance through a silicon addition), alloy 625LCF[®] (increased fatigue resistance through compositional and process optimization) and alloy 718 (increased high temperature strength through increased niobium content). This is to name but a few of the alloys derived from alloy 625.

It is of value to review the development history of alloy 625 because it gives one an insight into the interactions of key components of the alloy (9). The original intent for the alloy was a weldable, high creep strength, fabricable, non-age hardening tube alloy for steam service at 650°C. Using alloy 600 as a base, a series of molybdenum plus niobium heats were made and evaluated in creep testing at 52MPa/816°C to assess metallurgical strength and stability. The results pointed the way to significant age hardening and ultimately to the development of alloy 718. The aging response is shown in Figure 3.
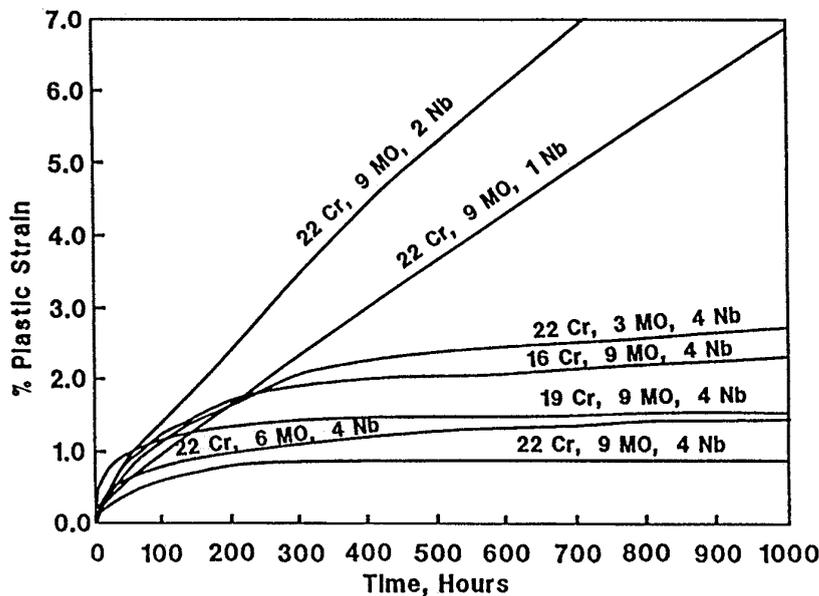

Figure 3: Creep Tests at 52 MPa/816°C for a range of niobium, molybdenum and chromium additions to nickel (9).

Custom Age 625 Plus[®] is a registered trademark of the Carpenter Technology Corporation. 625LCF[®] is a registered trademark of the Special Metals Corporation group of companies.

Because in the annealed condition these alloys possessed excellent fabricability, they could be easily made into standard mill products. However, it was believed that to commercialize the alloy, it would have better marketability if it were strong. Consequently the chromium and molybdenum levels were ultimately chosen to be 22% and 9%, respectively, as these levels did increase strength and enhance corrosion resistance as well.

Ultimately factorial experiments established the appropriate levels of niobium, molybdenum, chromium, aluminum and titanium. The niobium solubility in alloy 625 appears to be about 2.5% and increases with decreasing molybdenum plus chromium content (based upon a comparison of the aging response of alloy 718). See Figure 4.
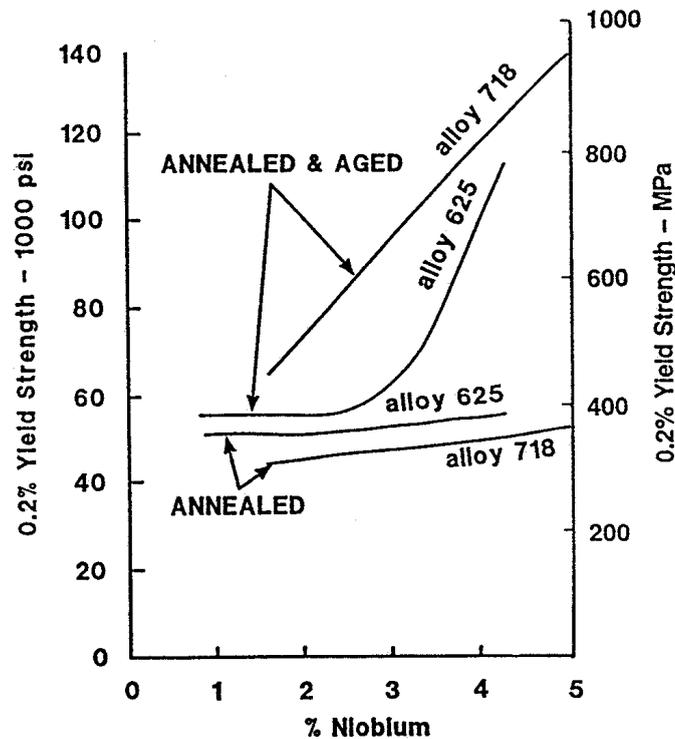

Figure 4: Effect of niobium additions on the 0.2% yield strength of the base compositions of alloys 625 and 718 (9).

This figure demonstrates only a slight matrix strengthening for alloy 625 as a function of niobium content in the annealed condition. However, in the aged condition (704°C/16h/AC) beginning at about 2.5% niobium there is a dramatic increase in yield strength. These studies noted that molybdenum increased the annealed strength of the matrix and may alone or in combination with niobium increase the age-hardening response and decrease the impact strength after high temperature exposure. Increasing chromium content from 16% to 22% increased annealed strength but did not markedly effect the aging response. Aluminum and titanium were kept low to minimize the aging response and promote weldability and braze-ability.

A time-temperature-transformation (TTT) diagram was first published by Schnabel, et al. in 1971 (10) and subsequently by Crum, et al. in 1981 (11) and lastly by Floreen et al. in 1994 (12) whose TTT diagram is shown in Figure 5. These TTT diagrams differ principally with respect to the precipitation of $M_{23}C_6$ and M_6C type carbides and may be related to differences in composition and grain size. Wang, et al. attribute minor differences in silicon and carbon content to the quantity and type of carbides in alloy 625 (13). Radavich and Fort reported their study on the stability of alloy 625 at intermediate temperatures (650°C to 870°C) and

confirmed the abundant formation of metastable coherent ordered γ'' phase (DO$_{22}$) in the matrix and its transformation to δ (Ni$_3$Nb) (orthorhombic DO$_a$) in the grain boundaries with extended exposure at 650°C (14). These authors also reported α-Cr in the grain boundaries and that it tended to increase with time at 650°C but failed to detect the phase at 760°C or 870°C. The γ'' was observed to coarsen at the grain boundaries and form intragranular platelets at 760°C. These platelets appear to be dissolving at 870°C while the grain boundary film appeared to be coalescing suggesting 870°C is near the δ solvus temperature.
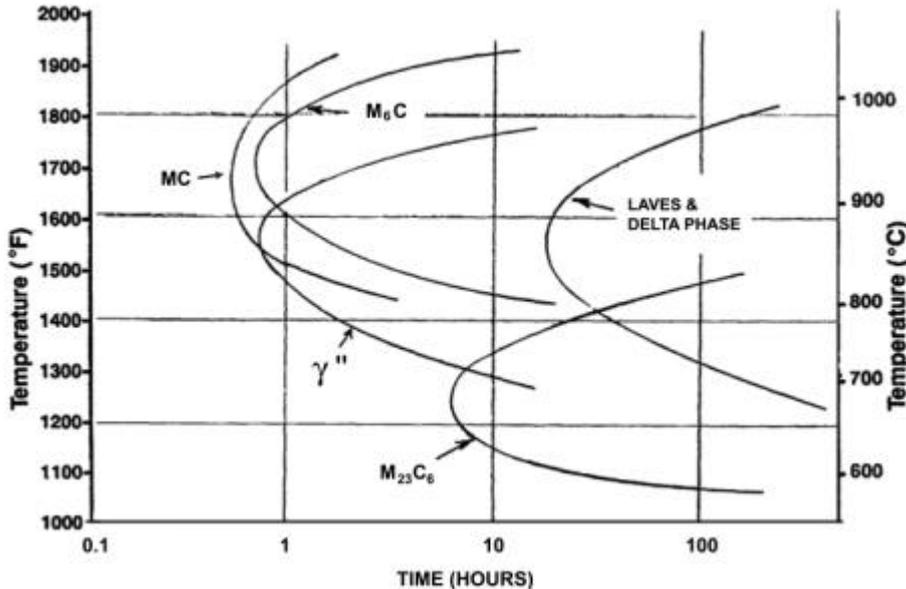

Figure 5: Suggested Time-Temperature-Transformation Diagram for alloy 625 (12).

Conder et al. exposed alloy 625 at 593°C and 650°C for times to 7,500 hours and then characterized the alloy for the phases present and evaluated the material for its room temperature and high temperature tensile properties (15). XRD and SEM examination revealed finely dispersed intragranular γ' and γ'' after 24h at 650°C and after 5,000h at 593°C. Further exposure at each temperature resulted in increasing amounts of each phase with a portion ultimately transforming to δ phase. The tendency for this transformation was more pronounced at the grain boundaries. Even after 7500h at either temperature, M$_{23}$C$_6$ type carbides was not detected confirming the earlier results of Beattie (3) and Sims (4) that niobium tends to stabilize MC carbides. However, MC and M$_6$C were found as predicted by the TTT diagrams of Schnabel et al. (10) and Crum, et al. (11) and Floreen et al. (12). Conder et al. confirmed the presence of α-Cr after 7,500h at 593°C and after 2,500h at 650°C at the grain boundaries. Floreen has recently summarized literature values for the chemical composition of the various phases found in alloy 625 (12). His results are presented in Table V.

Table VI presents the room temperature tensile properties of alloy 625 after aging at 593°C and 650°C for times to 24h and in Table VII for times to 7,500h. Table VIII lists the properties for each high temperature exposure for times to 7,500h. Table IX shows the restoration of original tensile properties after all exposures at both temperatures by the re-solutioning of the α-Cr, δ and γ'' phases at 954°C/1h/AC. The data presented are the average of two specimens per condition. Extended exposure at 593°C and 650°C show an increase in yield strength at 593°C up to 7,500h but a decrease after 5,000h at 650°C. Ductility is noted to decrease at both temperatures with time but remain greater than 20%.

Table V Structures and typical compositions of the precipitate phases that occur in alloy 625 as a result of thermal exposure (12)

Phase	Structure	Typical Composition
MC	Cubic, a = 0.43 å	Matrix blocky MC $(Ti_{0.07}Cr_{0.04}Fe_{0.02}Ni_{0.09}Nb_{0.75}Ni_{0.03})C$ $(Ti_{0.53}Cr_{0.03}Ni_{0.04}Nb_{0.39}Mo_{0.01})C$ Grain Boundary MC $(Ti_{0.15}Cr_{0.04}Fe_{0.01}Ni_{0.08}Nb_{0.67}Mo_{0.01})C$
M_6C	Cubic, a = 1.13 å	$(Cr_{0.21}Fe_{0.02}Ni_{0.37}Nb_{0.08}Mo_{0.24}Si_{0.08})_6C$
$M_{23}C_6$	Cubic, a = 1.08 å	$(Cr_{0.85}Fe_{0.01}Ni_{0.07}Mo_{0.07})_{23}C_6$
γ'	Ordered Tetragonal, a = 0.36, c = 0.74 å	$Ni_3(Nb_{>0.5}Ti_{<0.5}Al_{<0.5})$
δ	Orthorhombic, a = 0.51, b = 0.42, c = 0.45 å	Ni_3Nb
Laves	Hexagonal, a = 0.47, c = 0.77å	$(Cr_{0.31}Fe_{0.08}Ni_{0.41})_2(Si_{0.17}Ti_{0.01}Nb_{0.19}Mo_{0.63})$
$(Cr, Nb)_2N$	Tetragonal, a = 0.3, c = 0.77 å	$(Cr_{0.39}Ni_{0.07}Nb_{0.41}Mo_{0.13})_2N$

Table VI Room temperature tensile properties of alloy 625 after aging at 593°C and 650°C for various times

Aging Temperature	Aging Time Hours	Yield Strength MPa	Tensile Strength MPa	Elongation %
As-Annealed (1024°C/1h)		525	941	47
593°C	1	544	952	46
	4	560	969	45
	16	568	971	46
	24	583	978	45
650°C	1	559	983	46
	4	573	985	45
	16	679	1,050	40
	24	756	1,124	38

Table VII Room temperature tensile properties of alloy 625 after aging at 593°C and 650°C for various times

Aging Temperature	Aging Time Hours	Yield Strength MPa	Tensile Strength MPa	Elongation %
As-Annealed (1010°C/1h)		485	944	46
593°C	2500	890	1,257	29
	5000	935	1,296	27
	7500	1,029	1,342	22
650°C	2500	1,027	1,318	26
	5000	972	1,287	21
	7500	919	1,286	20

Table VIII High temperature tensile properties of alloy 625 after aging at 593°C and 650°C for various times.

Aging and Test Temperature	Aging Time Hours	Yield Strength MPa	Tensile Strength MPa	Elongation %
593°C	2500	734	1,050	30
	5000	839	1,143	27
	7500	907	1,183	22
650°C	2500	809	1,065	32
	5000	810	1,080	25
	7500	766	1,034	18

Table IX Room temperature tensile properties of alloy 625 after aging at 593°C and 650°C for various times followed by an anneal at 954°C/1h/air cool

Aging Temperature	Aging Time Hours	Yield Strength MPa	Tensile Strength MPa	Elongation %
As-Annealed (1010°C/1h/air cool)		485	944	46
593°C	2500	451	914	52
	5000	508	960	45
	7500	483	948	49
650°C	2500	474	964	49
	5000	503	970	45
	7500	490	956	49

Alloy 625 is generally recommended to be used at temperatures below 621°C. This is especially true for chemical, petrochemical and marine applications where long life and peak corrosion resistance are sought. For this service, alloy 625 is generally employed in the annealed condition where strength may be attributed mainly to solid solution strengthening, principally due to the alloy's molybdenum content but also from the niobium, chromium and carbon content to a lesser degree. Grain size as established by annealing conditions is noted to influence strength of annealed material as well (16).

While not found in fully homogenize wrought alloy 625, Laves phase is present in as-cast and welded microstructures. Heat treating at 1173°F effectively solutions this phase in alloy 625 (17). Higher levels of silicon, iron and niobium will tend to render solutioning this phase more difficult (12).

The Role of Niobium in Nickel-Iron Base Superalloys

A significant number of wrought superalloys strengthened with niobium are technically nickel-iron base alloys. Included in this grouping are such well known alloys as 706, 718, 903, and 909. Two of these alloys (alloys 706 and 718) have been selected for characterization. Their composition is given in Table I. These alloys have several features in common:

- These alloys are mainly used forged or wrought in applications up to temperatures not to exceed ~650°C.
- These alloys employ niobium for strengthening, frequently as the primary means of enhancing performance through precipitation of coherent γ' and γ'' phases.
- The amount of nickel must exceed 25% nickel to ensure a face-centered cubic (FCC) austenitic matrix in which γ' phase can precipitate.

Solid Solution Strengthening in Nickel-Iron Base Superalloys

As with the nickel-base superalloys, elements such as cobalt, chromium, molybdenum and tungsten along with niobium can lead to solid solution strengthening, although for niobium, precipitate phases play a more significant role. Stoloff estimated the level of niobium in solid solution in alloy 718 as ~3.0% (18). This would suggest that the contribution to strengthening in nickel-iron base superalloys is about the same as in the experimental nickel-base superalloys discussed above. Given that the mismatch between γ and γ' is not an important strenthening factor in nickel-base alloys, solid solution strengthening is not likely to be a major contributor to strength in nickel-iron base superalloys.

Carbide Strengthening by Niobium in Nickel-Iron Base Superalloys

The nickel-iron base superalloys form MC-type carbides. These carbides are important in controlling grain refinement during forging and heat treatment of this class of superalloys used widely as gas turbine discs and spacers. This carbide is generally titanium rich and generally complexed with niobium and the other refractory elements. Niobium helps stabilize the MC type carbide but it still can transform to $M_{23}C_6$ and M_6C type carbides upon subsequent high temperature heat treatment or thermal exposure.

Coherent Phase Strengthening by Niobium in Nickel-Iron Base Superalloys

There are two coherent phases, γ' and γ'', that form in nickel-iron base superalloys. The first of these phases, γ', is an ordered and coherent phase, formed by reaction of titanium with nickel. This is in contrast to the formation of γ' in nickel-base alloys by the reaction of nickel with aluminum. However, aluminum does participate, if present, along with titanium in forming γ' in the nickel-iron matrix. Gamma prime particles in a nickel-iron matrix are usually spherical and their volume fraction and size are critical in determining their contribution to strengthening. Paulonis has estimated the APB energy contribution to coherency strain is approximately 10 to 20% thereby discounting coherency strain as a important contributor to strength in these alloys. Gamma prime (γ') in the nickel-iron superalloy group of alloys can transform to γ'' as described below.

Because of the presence of niobium in nickel-iron base superalloys, gamma double prime, γ'', can be a prime contributor to strength. This coherent phase is body-centered- tetragonal (BCT) (it can be equated to two stacked FCC γ' cells in structure). It forms as discs or platelets within the matrix, has been observed to envelop γ' particles, and is apparently more stable than γ'. The phase depends on the presence of both niobium and iron, which provide the necessary electron-to- atom ratios and matrix to precipitate mismatch needed to form γ''. Figure 6 shows the quaternary phase relationships between γ, γ', γ'' and neighboring phases in the nickel, aluminum, niobium and chromium quaternary system.

While γ'' is more stable than γ', it in turn can transform to orthorhombic delta phase, δ (Ni_3Nb), depending on alloy composition and thermal exposure. The phase transformation sequence is as follows:

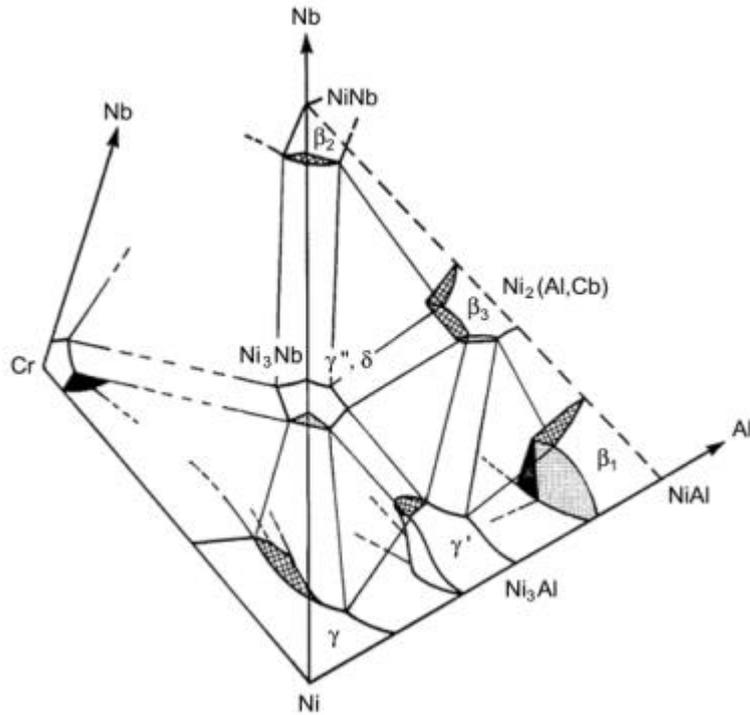$$\gamma' \text{ (FCC)} \rightarrow \gamma'' \text{ (BCT)} \rightarrow \delta \text{ (Orthorhombic)} \tag{2}$$

Figure 6: Sketch of the approximate relationships between γ, γ′, γ″ and δ in the nickel-aluminum-chromium-niobium system.

Delta phase is non-coherent with the matrix and forms as plates or cells. While it can contribute to grain control, its contribution to strength is doubtful (20). Another phase that can form directly from γ′ is eta phase, η (Ni$_3$Ti), due to high levels of titanium and niobium in the alloy. Eta phase usually occurs as plates or cells and is frequently found in grain boundaries where it dramatically reduces ductility. Certain heat treatments can lead to a more benign blocky form of the phase that can be used like δ to control grain size during fabrication. The formation of η and δ reduce potential strength since they both tie up titanium and niobium diminishing their availability to form γ′ and γ″.

Nickel-iron base superalloys can also form topographically closed-packed (TCP) phases and Laves. The presence of Laves is not uncommon and is related to the presence of niobium, iron and silicon in the alloy. While not related to the niobium content of these superalloys the formation of sigma, σ (Ni,FeCr) can occur in highly segregated microstructures or if the matrix is sufficiently deprived of nickel due to the formation of γ′, γ″, δ or η phases. The most important phases that can exist in nickel-iron base superalloys is summarized in Table X.

Table X Superalloy phases containing niobium

Name	Symbol	Structure	Chemical Formula
Gamma	γ	FCC	Solid Solution
Gamma Prime	γ′	Ordered FCC	Ni$_3$(Al,Ti,Nb)
Gamma Double Prime	γ″	Ordered BCT	Ni$_3$(Nb,Al,Ti)
Delta	δ	Orthorhombic	Ni$_3$(Nb$_8$Ti$_2$)
Eta	η	HCP	Ni$_3$(Ti,Nb)
MC Carbide	MC	Cubic	NbC
M$_6$C Carbide	M$_6$C	Complex Cubic	(Nb,Mo,Ni)$_6$C
Laves	---	Hexagonal MgZn$_2$	(Fe,Cr)$_2$(Ti,Nb)

Metallurgical Behavior of Niobium in Alloy 706

Alloy 706 evolved from the development of alloy 718 in the late 1960s to satisfy metallurgical requirements for large forged gas turbine components (21). Nickel, molybdenum and hardener content were lowered to enhance forgeability, reduce the tendency of the alloy range to develop macrosegregation in large cross sections, improve machinability and lower cost. Niobium and aluminum content were also reduced to decrease the tendency for segregation and freckle formation. The reduction of these hardeners necessitated an increase in the titanium content to maintain the alloy's strength characteristics. The carbon content was lowered from that in alloy 718 to aid machinability. The major phases and their typical morphologies found in alloy 706 are described in Table XI below.

Table XI Major precipitating phases present in alloy 706.

Precipitating Phase	Structure	Morphology	Composition
γ'	Ordered FCC	Spheres	$Ni_3(Al,Ti)$
γ''	Ordered BCT	Disks	Ni_3Nb
Laves	HCP	Globular	$(Fe,Ni)_2Nb$
η	HCP	Platelets/Cellular	Ni_3Ti
δ	Orthorhombic	Needles	Ni_3Nb

Gamma prime (γ') and γ'' are present in alloy 706 along with MC carbides, Laves and η phases (22). The principal strengthening phase is γ''. Heck has developed a TTT diagram for the alloy (23).
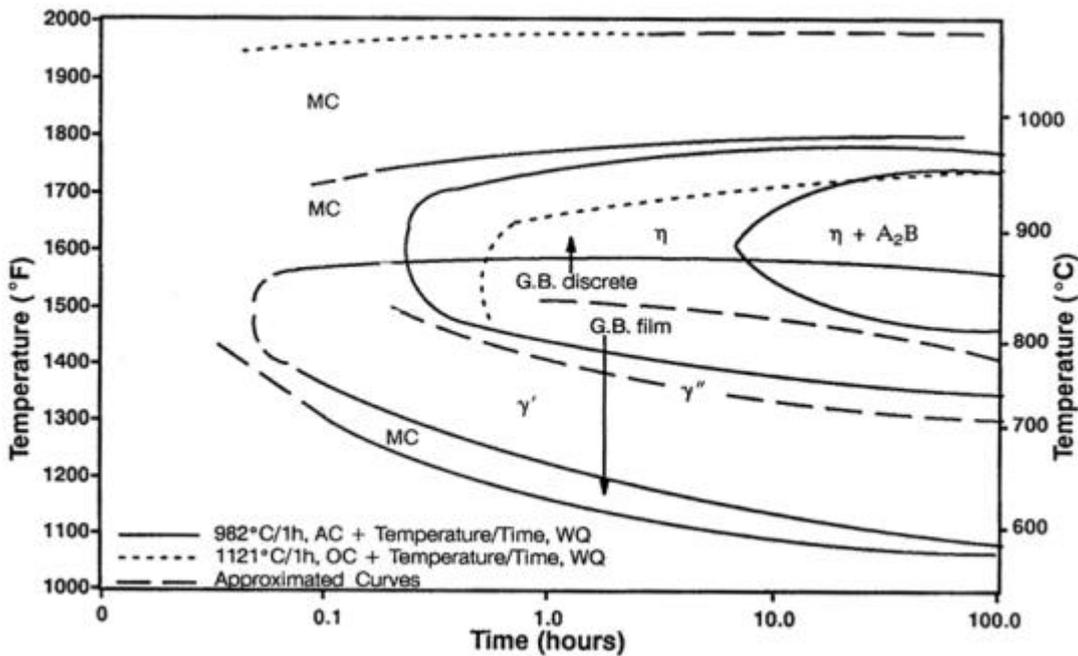

Figure 7: Approximate time-temperature-transformation diagram for alloy 706 (23).

To establish guidelines for forging, the re-solution temperatures for the common phases present in alloy 706 have been established (24). Both γ' and γ'' re-solution at ~885°C (slightly lower for longer times), phases η and δ at ~955°C (somewhat higher if the material is adversely segregated), grain boundary Laves at ~1065°C or higher if the particles are large. Moll, Maniar and Muzyka have presented an excellent review of the behavior of these phases during

processing and heat treatment (25). Numerous articles exist on the melting, processing and heat treatment of alloy and the interested reader is referred to these papers, since the focus here is on the role of niobium (26-30).

Gamma prime (γ') is the principal age hardening phase formed by isothermal heat treatment at and below ~700°C although it precipitates before γ'' at 760°C. It is generally spherical in shape and is an ordered $L1_2$ (a = 3.57 Angstroms) crystal structure. Extended exposure above ~650°C cause the γ' to transform to more stable η phase, in the form of coarse platelets, either in cellular colonies growing from grain boundaries or as an intragranular Widmanstatten structure. This transformation lowers strength.

Gamma double prime (γ'') is the predominate strengthening phase formed by heat treating between ~700°C and ~760°C although some γ'' will form over a broader temperature range. This phase is usually disc shaped and has an ordered BCT crystal structure. Gamma double prime (γ'') co-exists with the onset of titanium-rich η precipitation and appears to transform to η simultaneously with the appearance of γ' (22). Some investigators have reported the transformation of γ'' to coarse platelets of the stable orthorhombic (DO_a) δ phase with identical composition after long-term exposures above ~650°C. This phase can also form directly at higher temperatures (31).

The third precipitate of consequence in alloy 706 is eta phase, η (Ni_3Ti,Nb). This phase has a hexagonal DO_{24} crystal structure and appears as small platelets in grain boundaries and as thin lengthy platelets (needles) within the grains. It coarsens at the expense of γ' and γ'' between ~760°C and ~870°C. It nucleates uniformly within grains after an 1120°C anneal, but non-uniformly from lower annealing temperatures. This may be due to a remnant substructure related to prior precipitation of MC type particles since carbide formation appears to influence the η solvus temperature. There is compositional transition of γ'' (Ni_3Nb) [orthorhombic, DO_{22}] to η ($Ni_3Nb_{0.33}Ti_{0.67}$) [hexagonal, DO_{24}]. Eta phase can further transform with increasing titanium to η ($Ni_3Nb_{0.11}Ti_{0.89}$) [rhombohedral] to η ($Ni_3Nb_{0.03}Ti_{0.97}$) [hexagonal, DO_{24}. Precipitation of η to control grain size during forging is a common practice (24, 30, 32). Experience has shown than working alloy 706 below the η solvus temperature (~954°C) significantly increases flow stress and consequently forge press requirements. As recently as November, 2000, Balbach et al. patented a stabilizing step in the aging of alloy 706 for enhanced resistance to crack growth by heat treating after a 965 to 995°C/5-20h solution anneal at 775 to 835°C for 5 to 100h prior to the usual precipitation aging steps (33). The result of this stabilization heat treatment is the formation of substantial amounts of agglomerated η phase in the grain boundaries responsible for the inhibition of crack growth.

Alloy 706 will form Laves phase (Fe_2Nb) [hexagonal, C36 crystal structure] after extended exposure in the temperature range of about 870 to 930°C. Laves tends to look microstructurally like grain boundary η although somewhat coarser. Fesland and Petit studied the effect of silicon content on Laves phase formation in alloy 706 and presented the TTT diagram shown in Figure 8 for an alloy containing from 0.04 to 0.25% silicon (34). Kuhlman et al. confirmed the observations of Fesland and Petit in their study of the microstructure-mechanical property relationships in alloy 706 containing 0.07% silicon (35).

Niobium- and titanium-rich MC carbide (FCC, a = 4.43 Angstroms) form in alloy 706 as very fine precipitates mainly on grain boundaries during processing and aging heat treatments. Small amounts of $M_{23}C_6$, M_3C, NbN or Nb(C,N) type phases may occasionally be microstructurally observed.
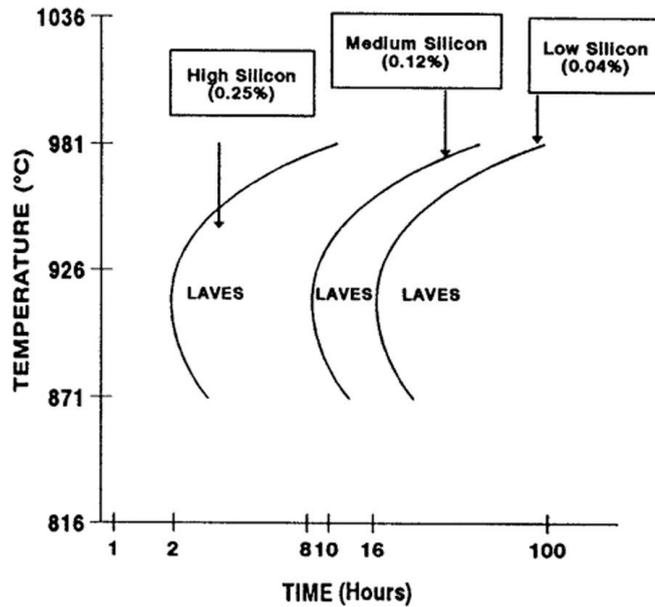
Figure 8: Time-Temperature-Transformation diagram showing the effect of silicon content on the formation of Laves phase in alloy 706 (34).

Optimum strength in alloy 706 is provided when a fine dispersion of γ''/γ' is formed in the alloy and subsequently stabilized. A common practice is 718°C/8h/AC, furnace cool at 55°C/h to 621°C/8h and then air cool. This procedure achieves excellent strength properties in less time with less likelihood of overaging to intragranular η than if a longer time isothermal heat treatment were used. Where maximum stress rupture strength is needed a third step of 843°C/3h is inserted between the anneal (optimally between 982 and 1010°C to avoid η and Laves phase formation) and the first aging step. This step, near the γ''/γ' solvus, precipitates discontinuous grain boundary η that improves notch ductility. Table XII presents typical forged properties taken from a heavy section forging after two step aging as described above (35).

TableXII Room temperature tensile properties of heavy section alloy 706 forging (35)

Location	Direction	Yield Strength, MPa	Ultimate Tensile MPa	Elongation %	Reduction In Area %	CVN Joules	ASTM Grain Size
Edge	L	1,068	1,268	21	39	67	4.1
Edge	T	1,041	1,261	19	36	61	4.0
Center	L	1,055	1,227	16	30	52	3.8
Center	T	1,041	1,193	16	29	35	3.9

Metallurgical Behavior of Niobium in Alloy 718

Alloy 718 is the predominant nickel-iron base superalloy. It represents almost half of the total tonnage of superalloy used throughout the world. The composition is shown in Table IV and the niobium-containing phases potentially present in the alloy are defined in Table XIII. It is made in virtually all product forms and is used for forged disks, shafts, supports, fasteners, sheet components and frame sections. The 53% nickel-20%iron matrix is strengthened mainly by 5.3% niobium that forms γ'' (~18 to 20%) giving alloy 718 higher yield strength than other superalloys strengthened by an equivalent amount of γ'. However, γ'', being metastable, tends

to transform to δ after long periods at temperatures at and above ~650°C resulting in some loss of strength (36-41).

Table XIII Niobium-containing phases in alloy 718 [Wlodek and Field (37)]

Phase	Structure	Analysis, at. %						
		Nb	Al	Ti	Fe	Cr	Mo	Si
γ	A1	1.97	0.74	0.52	23.8	22.0	2.41	0.64
γ′	L12	10.2	8.00	9.40	2.15	0.50	0.490	0.35
γ″	DO22	25.1	0.44	4.92	0.86	0.76	1.05	0.01
δ	DOa	20.4	0.80	3.00	5.30	3.40	2.20	0.10
Laves	C14	18.8	0.10	0.60	15.0	15.3	10.2	4.50
MC*	B1	14.6	0.10	80.0	0.90	1.90	0.50	1.90

*May contain nitrogen, also a high niobium form has been identified with 84 at.% Nb, 7 at.% Ti and small amounts of Fe, Ni and Cr.

Like alloy 706, alloy 718 precipitates γ″ as fine coherent platelets in the γ matrix. It is possible for the γ″ to surround cubic γ′ on all its six faces under certain thermal conditions and specific ratios of (Al + Ti)/Nb (42). This morphology has been proven to retard coarsening. Rizzo and Buzzanell have shown that increasing amounts of niobium from 3.5 to 6.5% steadily increase strength (43). However, above ~5%, niobium promotes Laves and δ that in alloy 718 are potentially deleterious to both toughness and strength. The composition of Laves phase typically ties up 28% of the niobium and 10% of the molybdenum contained in alloy 718 preventing these alloying elements to contribute to strength. Homogenization of the cast structure to eliminate Laves is difficult by heat treatment only. One technique to enhance homogenization and eliminate Laves has been described by Bouse and Schilke (44). They used a combination hot isostatic pressing (HIP) cycle plus heat treatment to minimize freckling and improve the yield strength from 780 to 920 MPa while retaining good ductility.

Numerous TTT diagrams have been described for alloy 718, one such diagram is shown in Figure 9 for wrought alloy 718 containing 5.38% niobium and 0.07% silicon (45).
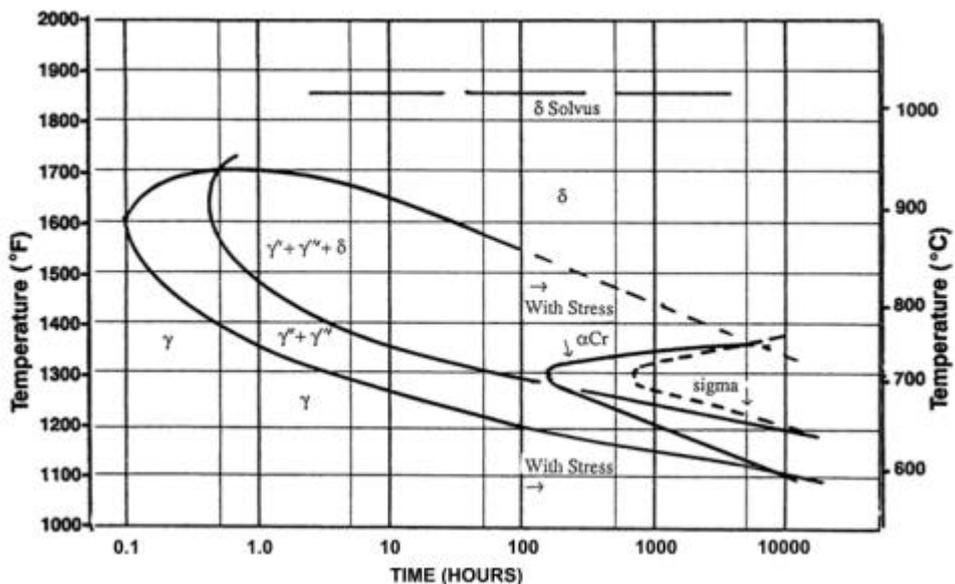

Figure 9: Time-Temperature-Transformation diagram for alloy 718 (45).

This diagram shows that in homogenized alloy 718 only γ', γ'' and δ are formed subsequent to hot working and an anneal at 1000°C/15 minutes. In this diagram, the primary carbides and any potential TiN are not depicted nor is Laves shown in confirmation of the results of Decker (46) and that of Brooks and Bridges (47). Interestingly, because the alloy contained alloy 0.07% silicon, the primary MC carbides did not transform to M_6C type carbides. The typical heat treatment requires an initial aging treatment at 720°C/8h, furnace cool to 620°C and hold for total aging time of 18 h followed by an air cool. This heat treatment defines the typical microstructure of alloy 718 in service usually at a temperature not in excess of 650°C. The γ'' forms readily at 720°C. Once the γ'' is precipitated, the γ' can form in the areas between the γ'' particles since the lower niobium content favors γ' formation. The precipitation of αCr as observed by Radavich after long term exposure or in shorter times under stress confirms the presence of these phases as reported by Wlodek and Field (37) and Brooks and Bridges (47). However, Radavich appears to be the first investigator to report the presence of σ phase.

Other diagrams such as those of Eiselstein (20) and Sims (4) depict the rapid formation of (Nb,Ti)C which over time transforms to $(Nb,Ti)_6C$. However, at typical use temperatures for alloy 718, it would appear that these carbides are relatively unstable and may decompose. Low carbon (0.008 to 0.027%) heats of alloy 718 have been studied by Jackman, et al. They report that at 0.008% carbon, stringers and clusters are eliminated and while grain growth became a problem to resolve, the fatigue, impact and fracture toughness improved substantially (48). Further, eliminating or minimizing niobium-rich carbides, frees niobium for strength enhancing phases.

Melting of Nickel-Iron Base Superalloys Containing Niobium-Bearing Phases

The production of a nickel-iron superalloy ingot typically begins with vacuum induction melting (VIM) of a consumable electrode. Vacuum melting minimizes oxygen and nitrogen pick-up by the heat and their reaction with the more reactive elements of the heat, particularly, aluminum, titanium and chromium. Vacuum arc remelting (VAR) is then commonly employed to further refine the heat, eliminate pipe and aid chemical uniformity. It is becoming increasing important to triple melt for maximum properties. The intermediate step is usually an electroslag remelt (ESR). There is a distinct trend towards the production of ever increasing diameter ingots to support the demand for larger diameter fan engines for aerospace and the larger rotors used in land-based gas turbines for electric power generation.

Due to the nature of these remelt processes and the characteristics of nickel-iron superalloys during melting, certain melt-related defects are common in alloys 706 and 718. These solute segregation defects are known as tree ring patterns, white spots and freckles (49).

Tree ring patterns are not considered detrimental to mechanical properties, which is not the case for white spots and freckles. White spots appear as light etching regions and are generally lower in alloying elements such as titanium and niobium. Jackman, Maurer and Widge have reported on the joint effort of producers, forgers and users to classify the types of white spots, determine their cause and effect on properties (50). White spots seem to be a consequence of VAR processing and require rigid process control to minimize (51). Freckles are defined by Wlodek and Field as areas of inverse segregation resulting from movement of rejected, solute rich, liquid in the mushy zone (liquid density inversion) and its entrapment (52). Freckles are promoted by slow melt rates, electromagnetic field disruptions and low thermal gradients. Freckling is aggravated in alloys 706 and 718 due to the large density difference between liquid and solid phases in the mushy zone, as well as by the low solute diffusivity and viscosity,

characteristic of the nickel-iron-niobium system. Freckles consist of phases high in concentration of the hardener elements. The 718 freckle is usually a semi-continuous longitudinal chain of Laves, outlining the grain boundaries with intragranular δ plates. Delta phase may be found within the Laves phase as can Nb-rich MC type carbides and high chromium M_3B_2 phases. Freckles are usually present in the mid-radial location of the ingot, though not exclusively, and may be associated with porosity. Because of their detrimental effect of fatigue properties, considerable research has been done to gain a better understanding of freckle formation during the VAR process and eliminate them through tighter process controls (53-55).

Processing of Nickel-Iron Base Superalloys Containing Niobium-Bearing Phases

Ingot processing begins with a thermal homogenization step to dissolve undesirable phases such as Laves and to reduce local compositional gradients, particularly those involving niobium and titanium. Homogenization and hot working furnace temperatures for alloys 706 and 718 typically range between 1100°C and 1200°C. Process modeling of ingot-to-billet conversion, particularly of the cogging operation, is becoming increasing sophisticated and more commonly practiced (56-59). Grain size receives particular attention.

As η was used by Balbach, et al., to improve the final properties of alloy 706 (33), Morra has employed δ formation in alloy 718 to aid large section forging by creating an extensive network of this phase prior to forging. The δ phase provides grain nucleation sites during forging to maintain grain size control (60). In their study, the precipitation was accomplished between 870°C and 915°C using times between 10 and 20h. Radavich studied the precipitation and growth of δ phase during hot working and found it to be an effective barrier to static recrystallization as it tends to precipitate intragranularly during hot working at temperatures between 870°C and 990°C (61). The δ phase will re-solution above ~1010°C and can result in re-precipitation as a continuous film in the grain boundaries, a condition that may be lead to embrittlement. An intriguing exploitation of the use of the ability of δ phase to control grain size is described in the paper by Smith and Flower in their development of a superplastic grade of alloy 718 that utilized extensive cold work plus multiple anneals in the δ phase region to produce a grain size of ASTM #10 or finer. At 950°C, this microstructure proved to be superplastic (62). Brown, Boettner and Ruckle developed a mini-grain rotary forge process by giving alloy 718 a short δ phase heat treatment to precipitate just enough δ phase to control grain growth (63).

The usual aging heat treatment for alloy 718 is 732°C/8h, furnace cool to 621°C and hold for 8h and air cool. The resultant mechanical properties are presented in numerous sources (4, 20, 62, 63, 64). An excellent summary is found in the Aerospace Structural Metals Handbook, Section 4103, January, 1995 edition.

Microstructural Characteristics of Niobium-Containing Weldments

Alloy 625 welding products are frequently used to both weld and overlay low and high alloyed steels, stainless steels and high temperatures nickel alloys because of its excellent welding characteristics. Numerous authors have reported on the microstructural characteristics of the weldments. Cortial, et al. on tungsten inert gas (TIG) weldments (65), Cieslak, et al. on gas0-tungsten-arc (GTA) weldments (66) and Hyatt et al. on electron beam weldments (67). All of these welding techniques tend to produce a similar microstructure in which niobium is very

much evident. The weldment is a cellular dentritic microstructure with directionally solidified columnar grains. There is gradient within the dentrite cores which constitutes the initial segregation within the solidifying weldment. A nominal composition of the dentrite core as measured on a TIG weldment is 60.8% nickel, 23.5% chromium, 7.8% molybdenum, 1.8% niobium, 4.3% iron and 0.35% silicon. The interdentritic area corresponds to the last liquid to freeze which quickly becomes an over saturated with niobium, molybdenum, titanium and silicon upon cooling leading to the precipitation of such minor phases as Laves, (NbMoTi)C and (MoNbTi)$_6$C carbides. A nominal composition of a TIG weldment interdentritic area is 58.6% nickel, 23.6% chromium, 9.0% molybdenum, 3.1% niobium, 3.7% iron and 0.6% silicon. Note the interdentritic enrichment in niobium, molybdenum and silicon. It is of interest to note that chromium does not appear to measurably segregate during solidification. Homogenization of alloy 625 weldments can be achieved above about 1000°C after 8 hours according to Cortial et al. (65). This is consistent with the results of Hyatt et al. as well (67).

The additional niobium content in alloy 718 promotes greater amounts of γ/Laves and γ/carbide eutectics in the weldment over that found in alloy 625. The presence of these low melting eutectics favors the retention of a liquid film between advancing dentrites that can contribute to solidification cracking. However, one of the principal features of alloy 718 is its improved weldability over that of γ′ strengthened alloys due to the sluggish precipitation kinetics of γ″. As a result, strain age cracking is avoided in subsequent post weld heat treatments. However, one of the drawbacks of welding alloy 718 is its tendency to form fissuring or solidification cracking in the heat-affected-zone (HAZ) in high restrain welds. An extensive list of references to solidification cracking in the HAZ is found in the article by Chaturvedi, et al. (68) This author found that high boron levels could be correlated with solidification cracking in electron beam welded cast alloy 718.

Effect of Niobium on the Long Term Stability of Alloy 718

Numerous authors have dealt with the long term stability of alloy 718, two of which have reported on times in excess of 10,000 hours at temperatures of 593°C and above (69,70). These authors have presented their view of the sequence of events as a function of time and temperature. Following the heat treatment for wrought alloy 718 of 980°C/1h + 620°C/8h, one finds the microstructure to contain the two precipitates, γ′ and γ″, the total amount being approximately 19% (69). The properties being largely determined by the γ″. Raising the temperature above 600°C leads to rapid γ″ growth and a gradual decline in mechanical properties. Above approximately 650°C, the γ″ begins to dissolve and is gradually replaced by δ. After 50,000h at 650°C, the grain boundaries are almost continuously decorated with δ phase. Only γ′ is found adjacent to the grain boundaries and in the interior of the grains the disk-shaped δ″ phase has grown from an initial precipitate size of 0.02 μm to 0.3 μm diameter. While the original size of the spheroidal γ′ is 0.01 μm, it is 0.06 μm diameter after exposure. After some 5,000h at 760°C, all γ″ is dissolved but some trace of γ′ can be found. The growing presence of δ leads to a demonstrative reduction on fatigue properties. Another degrading phenomenon also appears in the microstructure. Since chromium and molybdenum are sparingly soluble in δ, [Burke and Miller have measured the chromium content in δ and found it to contain only 3.4 weight % chromium (71)], these elements are rejected in advance of the growing δ platelets. The rejected chromium content leads to αCr formation and the rejected molybdenum to Laves and perhaps σ phase. αCr has been found in alloy 718 at temperatures as low as 593°C and in as short a time as 500h (72). αCr kinetics of nucleation and growth being strongly influenced by the degree of plastic deformation prior to exposure. The niobium content does play a role in the precipitation of these phases since the effect of niobium is to

change the delta solvus and volume fraction of the δ phase. Lindsley, et al., report that the formation of δ phase influences the formation of αCr by the constituent solute rejection mechanism described above and possibly by a mechanism whereby the δ phase provides an interface that lowers the nucleation energy below that of a grain boundary (73). However, this has yet to be proven, although it is true that αCr is frequently found adjacent to δ precipitates (74).

Conclusions

The contribution of niobium to the performance of superalloys is significant and the result of many of its fundamental characteristics (4). These are summarized below as are the unique ways that niobium enhance the properties of superalloys. The niobium phases that form in alloys 625, 706 and 718 are highlighted to define certain of their characteristics that these phases bring to superalloys.

1. The melting point and low modulus suggest limited benefit of niobium as a solid solution strengthener. Its large atom size mismatch with that of nickel and iron suggests limited solubility potential.

2. Niobium's electropositive position in the periodic table predicts the formation of stable carbides and nitrides. Thermodynamic considerations suggest niobium may compete with scale forming elements for surface oxide formation.

3. Atom size and electropositive position favor solubility of niobium in the phases, γ', γ'', η and δ.

4. Niobium readily concentrates in the γ' phase thereby adding to the total volume fraction of this phase by as much as 30%.

5. Niobium increases the APB energy of the γ' phase thereby increasing its resistance to dislocation cutting thus aiding high temperature strength.

6. The strong reaction of niobium with carbon to form NbC can be effectively utilized to control grain size, aid high temperature strength by reducing grain boundary slip and prevent MC plus γ phase degregation to $M_{23}C_6$ and γ' phase. In nickel alloys, up to 15-20% of the niobium presence partitions to the carbides.

7. In the presence of superalloys containing both nickel and iron, niobium forms γ'' phase leading to exceptional strength up to ~650°C. At higher temperatures over extended periods of time, γ'' phase will transform to δ phase, which does not contribute significantly to strength.

8. Delta (δ) phase in alloy 718 and η phase in alloy 706 can be effectively utilized to control grain size during mill processing and is the basis of certain mini-grain processing schemes and products.

References

(1) E. Guo and F. Ma, "The Strengthening Effect of Niobium in Ni-Cr-Ti Type Wrought Superalloy," <u>Superalloys 1980</u>, ed. J. K. Tien, (ASM Press, Metals Park, OH, 1980), 431-438.

(2) J. Mihalisin, C. G. Bieber and R. T. Grant, "Sigma-Its Occurrence, Effect and Control in Nickel-Base Superalloys," <u>Trans. AIME</u>, 242 (1968), 2399-2414.

(3) H. J. Beattie and W. C. Hagel, "Intragranular Precipitation of Intermetallic Compounds in Complex Austenitic Alloys," <u>Trans. AIME</u>, 221 (February 1967), 28-35.

(4) C. T. Sims, "A Perspective of Niobium in Superalloys," in <u>Niobium-Proceedings of the International Symposium</u>, ed. H. Stuart, (TMS, 1981), 1169-1220.

(5) G. Harris and N. Child, "Development of a High-Temperature Alloy for Gas-Turbine Rotor Blades", in <u>A Symposium on High Temperature Steels and Alloys for Gas Turbines,</u> (Iron and Steel Institute, London, July, 1952), 67-80.

(6) E. L. Raymond, "Mechanisms of Sensitization and Stabilization of INCOLOY alloy 825," (Paper presented at South Central Region NACE Conference, Denver, CO, October 16-19, 1967).

(7) O. Kriege and J. Baris, "The Chemical Partitioning of Elements in Gamma Prime Separated From Precipitation-Hardened, High-Temperature Nickel-Base Alloys", ASM <u>Trans.Quarterly,</u> March, 1969, 62, (1), 195-200.

(8) P. Thornton, et al., "The Temperature Dependence of the Flow Stress of the γ' Phase Based upon Ni_3Al", <u>Met. Trans.,</u> (1 January, 1970), 207-218.

(9) D. J. Tillack and H. L. Eiselstein, "The Invention and Definition of Alloy 625," <u>Superalloys 718, 625 and Various Derivatives</u>, ed. E. A. Loria, (TMS, Warrendale, PA, 1991), 1-14.

(10) E. Schnabel, H. J. Schuller and P. Schwaab, "The Precipitation and Recrystallization Behavior of the Nickel-Base Alloy INCONEL alloy 625," <u>Prakt. Metallographie,</u> 8 (1971), 521-527.

(11) J. R. Crum, M. E. Adkins and W. G. Lipscomb, "Performance of High Nickel Alloys In Intermediate Temperature Refinery and Petrochemical Environments," (Paper No. 208 at CORROSION 86, NACE, Houston, TX, 1986).

(12) S. Floreen, G. E. Fuchs and W. J. Yang, "The Metallurgy of Alloy 625," <u>Superalloys 718, 625 and Various Derivatives</u>, ed. E. A. Loria, (TMS, Warrendale, PA, 1994), 13-37.

(13) Y. S. Wang, X. M. Guan, H. Q. Ye, J. Bi and A. S. Xu, "Effect of Silicon on Grain Boundary Carbide Precipitation and Properties of a Cobalt-Free Wrought Nickel-Base Superalloy," <u>Superalloys 1980</u>, ed. J. K. Tien, (ASM, Metals Park OH, 1980), 63-70.

(14) J. F. Radavich and A. Fort, "Effects of Long-Time Exposure in Alloy 625 at 1200°F, 1400°F and 1600°F," <u>Superalloys 718, 625, 706 and Various Derivatives</u>, ed. E. A. Loria, (TMS, Warrendale, PA, 1994), 635-647.

(15) C. R. Conder, G. D. Smith and J. F. Radavich, "Microstructural and Mechanical Property Characterization of Aged INCONEL alloy 625LCF," Superalloys 718, 625, 706 and Various Derivatives, ed. E. A. Loria, (TMS, Warrendale, PA, 1997), 447-458.

(16) G. D. Smith, J. R. Crum and R. A. Smith, "Alloy Optimization for Enhanced Flexible Coupling Performance," (Paper No. 960578, SAE Int'l, Warrendale, PA, 1996).

(17) M. J. Cieslak, "The Welding and Solidification Metallurgy of Alloy 625", Weld Journal, 70 (1991), 49s-56s.

(18) N. Stoloff, "Fundamentals of Strengthening" The Superalloys, (Wiley-Interscience, New York, 1972), 79-112.

(19) D. Paulonis, et al., "Precipitation in Nickel-Base Alloy 718", Trans. ASM, 62 (1969), 611-622

(20) H. L. Eiselstein, "Metallurgy of a Columbium-Hardened Nickel-Chromium-Iron Alloy," ASTM STP No. 369, (ASTM, Philadelphia, PA 1965), 62-79.

(21) H. L. Eiselstein, "Properties of INCONEL alloy 706," (Presented at Materials Engineering Congress, Cleveland, OH 1970).

(22) L. Remy, J. Laniesse and H. Aubert, "Precipitation Behavior and Creep Rupture of 706 Type Alloys, Materials Science and Engineering, 38 (1979), 227-239.

(23) K. A. Heck, "The Time-Temperature-Transformation Behavior of Alloy 706," Superalloys 718, 625, 706 and Various Derivatives, ed. E. A. Loria, (TMS, Warrendale, PA, 1994), 393-404.

(24) D. R. Muzyka and G. N. Maniar, "Microstructure Approach to Property Optimization in Wrought Superalloys," ASTM STP 557, (ASTM, Philadelphia, PA 1974), 198-209.

(25) J. H. Moll, G. N. Maniar and D. R. Muzyka, "The Microstructure of 706, A New Fe-Ni-Base Superalloy," Metallurgical Transactions, 2, (8) (August, 1971), 2143-2151.

(26) A. M. Johnson and K. E. Fritz, "Properties and Microstructure of a Large Forged Superalloy Turbine Wheel," Superalloys – Metallurgy and Manufacture, Proceedings of the 3rd Intn'l Symposium, ed. B. H. Kear et al., (Published by Claitor's Publishing Division, Baton Rouge, LA, 1976), 25-35.

(27) F. S. Suarez, J. E. Roberts and L. D. Schley, "Ingot Optimization in a Superalloy – INCONEL alloy 706," Presented at Fifth Int'l Symposium on Electroslag and Other Special Melting Technologies, (Carnegie-Mellon Institute of Research, Pittsburgh, PA, 1975), 126-149.

(28) P. W. Schilke, J. J. Pepe and R. C. Schwant, "Alloy 706 Metallurgy and Turbine Application," Superalloys 718, 625, 706 and Various Derivatives, ed. E. A. Loria, (TMS, Warrendale, PA, 1994), 1-12.

(29) S. V. Thambo, "Melt Related Defects in Alloy 706 and Their Effects on Mechanical Properties," ibid., 237-152.

(30) C. P. Sullivan and M. J. Donachie, "Microstructures and Mechanical Properties of Iron-Base (Containing Ni) Superalloys," Metals Engrg Quarterly, November, 1971, 1-11.

(31) R. Cozar and A. Pineau, "Morphology of γ' and γ'' Precipitates and Thermal Stability of INCONEL alloy 718 Type Alloys, Metall. Trans., 4 (1973), 47-59.

(32) D. R. Muzyka, "Controlling Microstructures and Properties of Superalloys Via Use of Precipitated Phases," Metals Engrg Quarterly, November 1971, 12-19.

(33) W. Balbach, G. Harkegard and R. Redecker, "Heat Treatment Process for Material Bodies Made of a High Temperature Resistant Iron-Nickel Superalloy and Heat Treatment Material Body," U. S. Patent #6,146,478, November 14, 2000.

(34) J. P. Fesland and P. Petit, "Manufacturing Alloy 706 Forgings," Superalloys 718, 625, 706 and Various Derivatives, ed. E. A. Loria, (TMS, Warrendale, PA, 1994), 229-248.

(35) G. W. Kuhlman, A. K. Chakrabarti, R. A. Beaumont, E. D. Seaton and R. F. Radavich, "Microstructure-Mechanical Properties Relationships in INCONEL alloy706 Superalloy," ibid., 441-450.

(36) A. Oradei-Basile, and J. F. Basile, "A Current T.T.T. Diagram for Wrought Alloy718," Superalloys 718, 625, 706 and Various Derivatives, ed. E. A. Loria, (TMS, Warrendale, PA, 1991), 325-335.

(37) S. T. Wlodek and R. D. Field, "The Effects of Long Time Exposure on Alloy 718," Superalloys 718, 625, 706 and Various Derivatives, ed. E. A. Loria, (TMS, Warrendale, PA, 1994), 659-670.

(38) J. H. Davidson, "The Structural Stability of High Temperature Alloys," Presented at Course on The Structure of High Temperature Alloys, (PETTEN Institute, The Netherlands).

(39) C. I. Garcia, A. K. Lis, E. A. Loria and A. J. DeArdo, "Thermomechanical Processing and Continuous Cooling Transformation Behavior of Alloy 718," Superalloys 1992, ed. S. D. Antolovich, et al., (TMS, Warrendale, PA, 1992), 527-536.

(40) R. Cozar, M. Rouby, B. Mayonobe, C. Morizot, "Mechanical Properties, Corrosion Resistance and Microstructure of Both Regular and Titanium Hardened 625 Alloys," Superalloys 718, 625 and Various Derivatives, ed. E. A. Loria, (TMS, Warrendale, PA, 1991), 423-436.

(41) W. J. Boesch and H. B. Canada, "Precipitation Reactions and Stability of Ni_3Cb in INCONEL alloy 718", Journal of Metals, 21 (October, 1969), 34-38.

(42) T. Shibata, Y. Shudo, T. Takahashi, Y. Yoshino and T. Ishiguro, "Effect of Stabilizing Treatment on Precipitation Behavior of Alloy 706," Superalloys 1996, ed. R. D. Kissinger, et al., (TMS, Warrendale, PA, 1996), 627-634.

(43) F. Rizzo and J. Buzzanell, "Effect of Chemistry Variations on the Structural Stability of Alloy 718", Journal of Metals, 21 (1969), 24-33.

(44) G. Bourse and P. Schilke, "Process Optimization of Cast Alloy 718 for Water Cooled Gas Turbine Application", <u>Proc. Fourth Int'l Conference on Superalloys</u>, (ASM Press,Metals Park, OH, 1980), 303-310.

(45) A. Oradei –Basile and J. F. Radavich, "A Current T-T-T Diagram for Wrought Alloy 718." <u>Superalloys 718, 625 and Various Derivatives</u> , ed. E. A. Loria, (TMS, Warrendale, PA, 1991), 325-336.

(46) R. F. Decker, "Strengthening Mechanisms in Nickel-Base Superalloys," presented at <u>The Steel Strengthening Mechanisms Symposium</u>, (Zurich, Switzerland, 1969).

(47) J. W. Brooks and P. J. Bridges, "Metallurgical Stability of INCONEL alloy 718," <u>Superalloys 1988</u>, ed. S. Reichman, et al., (TMS, Warrendale, PA, 1988), 33-42.

(48) L. A. Jackman, M. D. Boldy and A. L. Coffey, " The Influence of Reduced Carbon on Alloy 718," <u>Superalloys 718, 625 and Various Derivatives</u>, ed. E. A. Loria, (TMS, Warrendale, PA, 1991), 261-270.

(49) L. W. Lherbier, "Melting and Refining," <u>Superalloys II</u>, ed. C. T. Sims, N. S. Stoloff and W. C. Hagel, (published by John Wiley & Sons, New York, 1987), 403-405.

(50) L. A. Jackman, G. E. Maurer and S. Widge, "White Spots in Superalloys," <u>Superalloys 718,625,706 and V. Derivatives</u>, ed. E. A. Loria, (TMS, Warrendale, PA, 1994), 153-166.

(51) K. O. Yu, J. A. Dominque, G. E. Maurer and H. D. Flanders, "Macrosegregation in ESR and VAR Processes," <u>Journal of Metals</u>, 38 (1) (1986), 46-48.

(52) S. T. Wlodek and R. D. Field, "Freckles in Cast and Wrought Products," <u>Superalloys 718,625,706 and Var. Derivatives</u>, ed. E. A. Loria, (TMS, Warrendale, PA, 1994), 167-176.

(53) P. D. Genereux and C. A. Borg, "Characterization of Freckles in a High Strength Wrought Nickel Superalloy," <u>Superalloys 2000</u>, ed. T. M. Pollock, et al., (TMS, Warrendale, PA., 2000), 19-27.

(54) J. A. Van Den Avyle, J. A. Brooks and A. C. Powell, "Reducing Defects in Remelting Processes for High Performance Alloys," <u>Journal of Metals</u>, 50 (3) (1998), 22-25.

(55) J. M. Moyer, L. A. Jackman, C. B. Adasczik, R. M. Davis and R. Forbes-Jones, "Advances In Triple Melting Superalloys 718, 706 and 720," <u>Superalloys 718, 625, 706 and Various Deviratives</u>, ed. E. A. Loria, (TMS, Warrendale, PA, 1994), 43-45.

(56) C. A. Dandre, C. A. Walsh, R. W. Evans, R. C. Reed and S. M. Roberts, "Microstructural Evolution of Nickel-Base Superalloy Forgings during Ingot-to-Billet Conversion: Process Modeling and Validation," <u>Superalloys 2000</u>, ed. T. M. Pollock, et al., (TMS, Warrendale, PA, 2000), 85-94.

(57) B. F. Antolovich and M. D. Evans, "Predicting Grain Size Evolution of Udimet[®] alloy 718 During the "Cogging" Process through Use of Numerical Analysis," <u>Superalloys 2000</u>, ed. T. M. Pollock, et al., (TMS, Warrendale, PA, 2000), 85-94.

(58) R. A. Jaramillo, F. S. Suarez, J. A. Plyburn and D. E. Camus, "Evaluation of an INCONEL Alloy 718 Microstructural Evolution Model," <u>Superalloys 718, 625, 706 and Various Derivatives,</u> ed. E. A. Loria, (TMS, Warrendale, PA, 1997), 257-266.

(59) C. Boyko, H. Henein and F. R. Dax, "Modelling of Open Die and Radial Forging Processes for Alloy 718," <u>Superalloys 718, 625 and Various Derivatives</u>, ed. E. A. Loria, (TMS, Warrendale, PA, 1991), 107-124.

(60) M. M. Morra, "Delta-Phase Grain Refinement of Nickel-Iron-Base Alloy Ingots," U. S. Patent #6,193,823 B1, February 27, 2001.

(61) J. F. Radavich and W. H. Couts, Jr., "Factors Affecting Delta Phase Precipitation and Growth at Hot Work Temperatures for Direct Aged INCO 718," <u>Superalloys 1984</u>, ed. M. Gell et al., (TMS, Warrendale, PA, 1984), 497-507.

(62) G. D. Smith and H. L. Flower, "Superplastic Forming of INCONEL alloy 718," <u>Superalloys 718, 625 and Various Derivatives</u>, ed. E. A. Loria, (TMS, Warrendale, PA, 1994_, 355-364.

(63) E. E. Brown, R. C. Boettner and D. R. Ruckle, "Minigrain Processing of Ni-Based Alloys," <u>SUPERALLOYS—PROCESSING, Proceedings of the Second International Conference,</u> (TMS, Warrendale, PA, 1972), L1 – L12.

(64) INCONEL alloy 718, <u>Technical Bulletin</u>, Special Metals Corporation, 2000.

(65) F. Cortial, J-M. Codrieu and C. Vernot-Loier, "Heat Treatments of Weld Alloy 625: Influence on the Microstructure, Mechanical Properties and Corrosion Resistance," <u>Superalloys 718, 625 and Various Derivatives</u>, ed. E. A. Loria, (TMS, Warrendale, PA, 1994), 859-870.

(66) M. J. Ciesak, T. L.. Headley, T. Lollie, A. D. Romig, Jr., "A Melting and Solidification Study of Alloy 625," <u>Met. Trans. A</u>, 19A (September 1988), 2319-2331.

(67) B. Z. Hyatt and C. M. Brown, "Microstructure and Mechanical Properties of Stress Relieved Electron Beam Welded Alloy 625," <u>Superalloys, 718, 625, 706 and Derivatives,</u> Ed. E. A. Loria, (TMS, Warrendale, PA, 2001), 645-656.

(68) M. C. Chaturvedi, W. Chen, A. Saranchuk, "The Effect of B Segregation on Heat-Affected Zone Microfisssuring in EB Welded INCONEL 718," <u>Superalloys, 718, 625, 706 and Derivatives,</u> Ed. E. A. Loria, (TMS, Warrendale, PA, 1997), 743-752.

(69) S. T. Wlodek, "The Stability of Superalloys," <u>Long Term Stability of High Temperature Materials,</u> ed. G. E. Fuchs, K. A. Dannemann and T. C. Deragon, (TMS, Warrendale, PA, 1999).

(70) J. F. Radavich, "Long Time Stability of a Wrought Alloy 718 Disk," <u>Superalloy 718 – Metallurgy and Applications,</u> ed. E. A. Loria, (TMS, Warrendale, PA, 1989), 257-268.

(71) M. G. Burke and M. K. Miller, "Precipitation in Alloy 718: A Combined AEM and APFIM Investigation," <u>Superalloys 718, 625 and Various Derivatives,</u> ed. E. A. Loria, (TMS, Warrendale, PA, 1991), 337-350.

(72) J. F. Radavich and B. A. Linsley, "Effect of Residual Strain on Alpha CR Precipitation in Alloy 718 Fasteners," <u>Superalloys 718, 625, 706 and Various Derivatives</u> ed. E. A. Loria, (TMS, Warrendale, PA, 2001), 411-420.

(73) B. A. Lindsley, X. Pierron, G. E. Maurer, "α-Cr Formation in Alloy 718 During Long Term Exposure: The Effect of Chemistry and Deformation," ed. G. E. Fuchs, K. A. Dannemann and T. C. Deragon, (TMS, Warrendale, PA, 1999), 23-133.

(74) X. Xie, G. Wang, J. Dong, C. Wu, J. F. Radavich, G. Shen and B. A. Lindsley, "Alpha Chromium Formation in Alloy 718 and It's Effect of Creep Crack Propagation," <u>Superalloys 718, 625, 706 and Various Derivatives</u>, ed. E. A. Loria, (Warrendale, PA, 2001), 399-410.